CSM Instruments
Advanced Mechanical Surface Testing

APPLICATIONS BULLETIN

Influence of indenter tip radius on the scratch resistance of an automotive clearcoat

Methods for characterizing the mechanical properties of automotive polymeric clearcoats have seen extensive development over the last few years [1-3] and have led to the first dedicated ASTM standard [4] which is based on the Nano Scratch Tester. This standard follows on from previous methods used in evaluating scratch and mar, where the objective was to physically scratch the surface and then use visual inspection to assign a ranking. Although useful, some methods do not have the accuracy or reproducibility of the nano scratch test method, which allows investigation of the relationship between damage shape and size, and external input (such as applied load, indenter geometry, speed, etc.)

Mar resistance (also featured in Applications Bulletin No. 7, April 1998 and No. 15, Oct. 2000) characterizes the ability of the coating to resist damage caused by light abrasion. The difference between mar and scratch resistance is that mar is related only to the relatively fine surface scratches which spoil the appearance of the coating. Mar resistance therefore directly relates to the level of gloss retention in the coating after exposure of the material to harsh environmental conditions. Typical conditions include daily and seasonal fluctuations of temperature and humidity, acid rain and salt exposure, car washing and road grit. Traditional nano scratch testing methodologies have focused on simulation of mar-type damage, which consists of small width scratches (typically < 10 µm) and shallow depths (typically < 10 µm) which both require small indenter radii (typically < 5 µm) to achieve. Although very useful for characterizing mar-type damage, the scratch test method can also be used to simulate other types of damage which may occur on an automotive topcoat during the lifetime of the vehicle. Such damage might be caused by keys or jewellery being scraped across the surface, or by large particle impact (gravel from the road), both of which cause large-scale damage which is obviously visible to the human eye regardless of paint color and light level. Simulation of larger scale damage requires the use of larger sized spherical indenter tips and higher applied loads.

This application note focuses on the influence of indenter tip radius on the scratch resistance by varying tip radius and investigating the resultant variations in measured signals and the effect on the physical damage of the polymeric coating, especially the critical point at which fracture of the coating occurs. It is widely known that the critical point can depend on the scratch speed, temperature, the amount of deformation (strain) and the deformation history. The indenter tip creates a complex distribution of stresses and strains around its contact which are directly influenced by the size and shape of the tip as well as the rheological properties of the polymer. ASTM D7187 defines the onset of fracture as the point where the normal force, tangential force and penetration depth begin to fluctuate wildly, this being also commonly known as the critical failure load, Lc1. However, it has been found that in some polymer topcoats, the exact fracture point is difficult to determine due to the particular formulation and the way that fracture initiates. One way to "amplify" this transition from plastic deformation to fracture is to observe the normal load measured during the post-scan phase of the test.

The post-scan consists of running the indenter along the scratched track with a very low load in order to measure the residual depth remaining after the scratch test. This normal load signal, known as FnP, can provide a particularly good indicator of fracture even when the depth signals do not show a marked transition. Fig. 1 shows a typical example of a progressive load scratch on an automotive polymer topcoat where the FnP signal is a clear indicator of coating fracture.

In order to investigate the influence of indenter tip radius on the scratch resistance, it was important to choose a polymeric topcoat material whose mechanical properties are well known. For this reason it was decided to use a common automotive polymeric topcoat known as GEN III. This material has a very reproducible critical fracture point at ~ 9 mN when scratched with a 2 µm radius indenter and so seemed an ideal candidate for comparative testing. It is interesting to note that the CSM Instruments Applications Lab has had a sample of GEN III which was stored in ambient conditions for over 10 years and still gives exactly the same critical fracture point. It can therefore be concluded that after initial curing, this material remains stable if not exposed to ultraviolet radiation and significant temperature fluctuation.

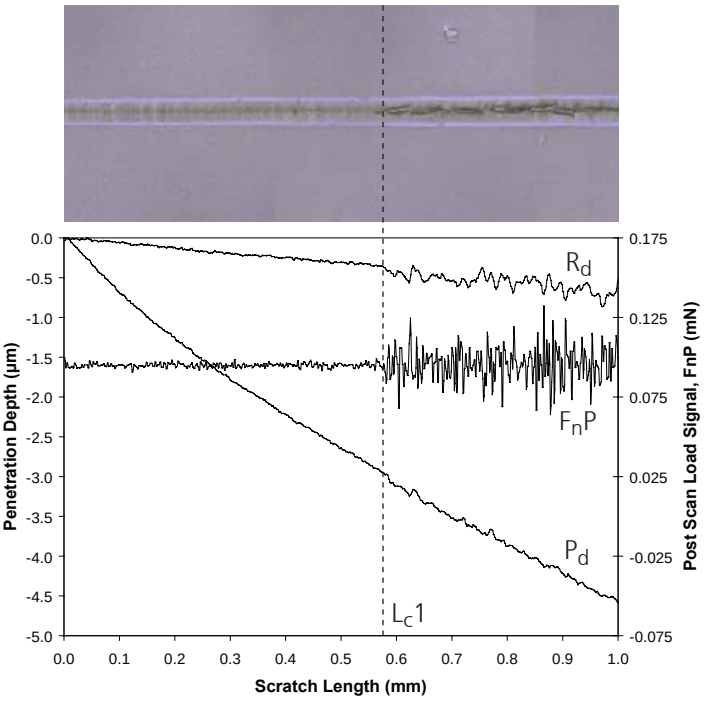

Figure 1: Nano Scratch Tester results for a progressive load scratch (0.1 – 15 mN) on a GEN III automotive polymer topcoat showing the penetration depth (Pd), residual depth (Rd) and normal load during post-scan (FnP) signals. The onset of fracture (Lc1) is clearly visible (shown here as a dotted line) and corresponds exactly with the optical micrograph shown of the scratch around the fracture point.

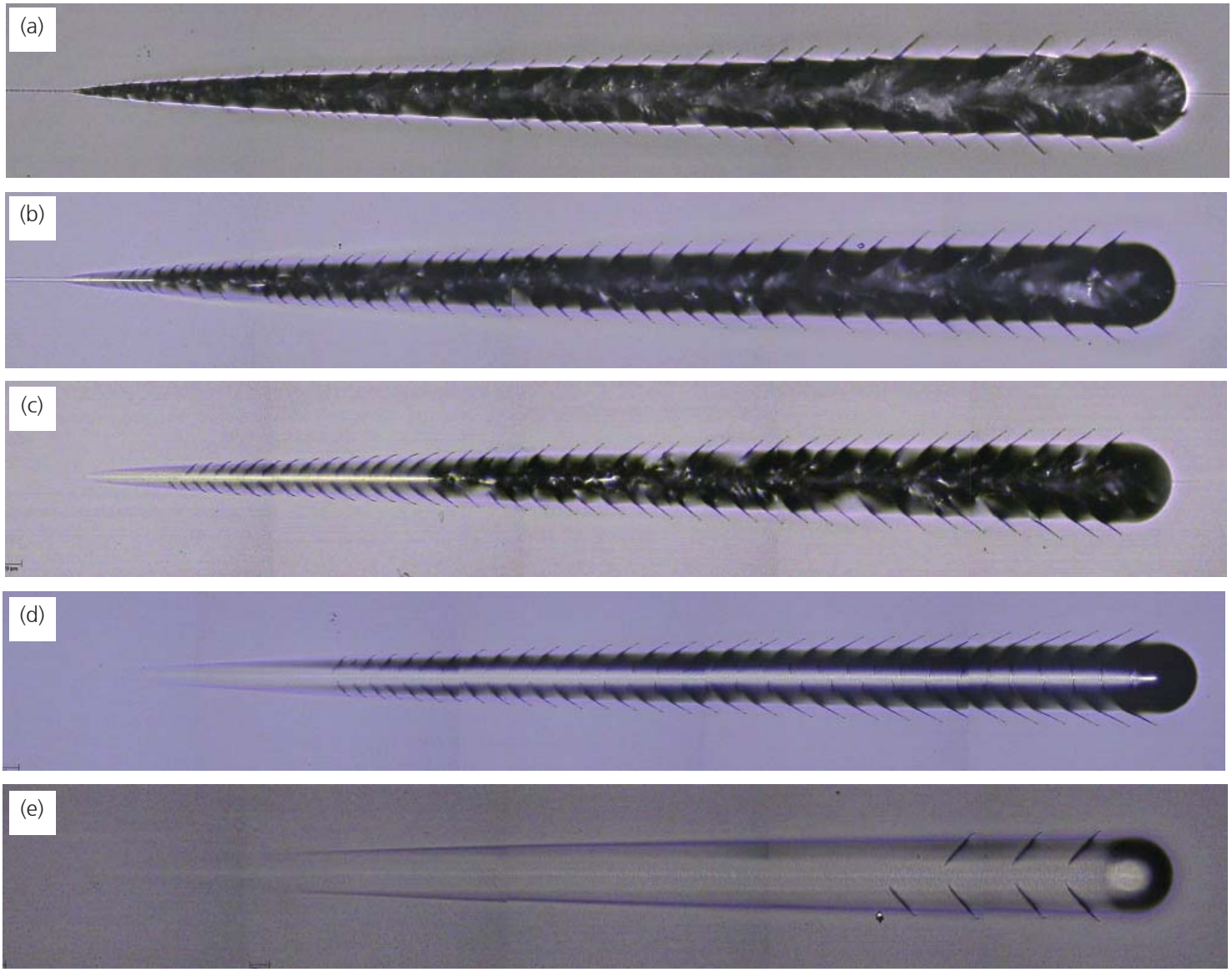

Figure 2: Scratches made on a GEN III polymer topcoat with the following spherical indenter radii; (a) 2 µm; (b) 5 µm; (c) 10 µm; (d) 20 µm; (e) 50 µm. Scratch test conditions were identical in each case, namely applied load 1 – 600 mN, speed 0.5 mm/min., loading rate 300 mN/min. and scratch length 1 mm.

It was decided to cover indenter tip radii from 2 µm up to 50 µm, this being the widest range of radius possible with one machine (in this case the Nano Scratch Tester, whose applied load covers the range of 0.01 – 1000 mN). By trial and error it was found that 1 – 600 mN was the ideal load range for the 5 indenter geometries and a complete scratch made with each is shown in Fig. 2. Initial observation of these scratch tracks suggests that there are two different modes of failure, the first being chevron-cracking along the sides of the scratch, the second being the onset of full fracture within the scratch. The best example of these two modes is the 10 µm indenter radius scratch in Fig. 2 (c) where cracking commences at 51 mN and full fracture at 184 mN.

The only other indenter to show both failure modes is the 5 µm radius where cracking commences at 28 mN and full fracture at 52 mN. For the smallest radius (2 µm), full fracture occurs so soon after the start of the scratch that it is not possible to observe the transition. However, it is known from standard testing of this material with a 2 µm indenter that failure (both cracking and fracture) occurs at ~ 9 mN. For the larger radii indenters, only cracking is observed, this occurring at 146 mN for the 20 µm radius and 492 mN for the 50 µm radius.

It is interesting to note that all the indenters used in the range 2 – 50 µm had a cone angle of 90°, this meaning that once the penetration depth of the scratch exceeds the radius of the indenter then the sidewalls of the cone are going to exert a greater influence on the material deformation than the actual radius of the tip. However, the sidewalls had no effect on the first critical failure point (Lc1) because the penetration depth at Lc1 was always lower than the indenter radius, as shown in Fig. 4. The plotted data in this graph suggests a linear dependence between indenter radius and penetration depth at Lc1.

The strain rate during a scratch test can be defined as the ratio V/a, where V is the scratch speed and a is the scratch width. Because the scratch speed was maintained constant in all tests (0.5 mm/min., or 8.33 µm/s) the strain rate dropped from 2.16 s^{-1} for the 2 µm indenter, to only 0.11 s^{-1} for the 50 µm indenter. This evolution is also plotted as a function of indenter radius in Fig. 4. This drastic reduction in strain rate helps to explain why there is far less damage with the 50 µm indenter than with the 2 µm indenter. This brings to light one of the most important characteristics of automotive polymer coatings, which is the dependence of their behaviour on the rate at which the

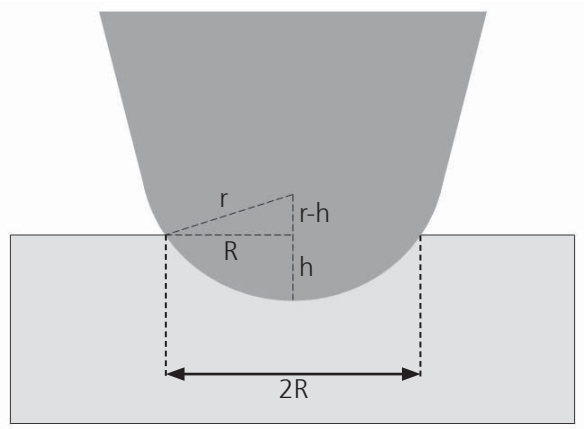

Figure 3: Cross-section through a spherical indenter of radius r which is scratching through a material to a depth h. The width of the scratch is therefore given by the distance 2R.

strains are applied. These viscoelastic characteristics of the polymer greatly influence how the material deforms under the indenter tip, and how it recovers after the deformation has occurred. The scratch width, a, is calculated from the following equation where a = 2R:

$$R^2 = r^2 - (r - h)^2$$

The parameters are shown in Fig. 3 and are defined based on the spherical indenter radius, r, and the scratch depth at the first critical load (Lc1), given by h.

Fig. 5 shows overlay plots for the Pd, Rd and Ft signals for the 5 scratches shown in Fig. 2. The penetration depth overlays (a) seem to scale with indenter radius with the maximum depth from the 2 µm radius and the minimum depth from the 50 µm. The same trend is observed with the residual depth plots (b) with the sharpest indenter causing the noisiest residual profile owing to the significant increase in damage to the surface. These plots make the most sense when compared with the micrographs shown in Fig. 2 where the onset of damage correlates well between observed fracture and the recorded signals. The friction force overlays (c) rank the 2 µm radius with the highest frictional component and the 50 µm radius with the lowest. This makes sense when it is considered that the sharper indenters are scratching far deeper than their actual radius and thus

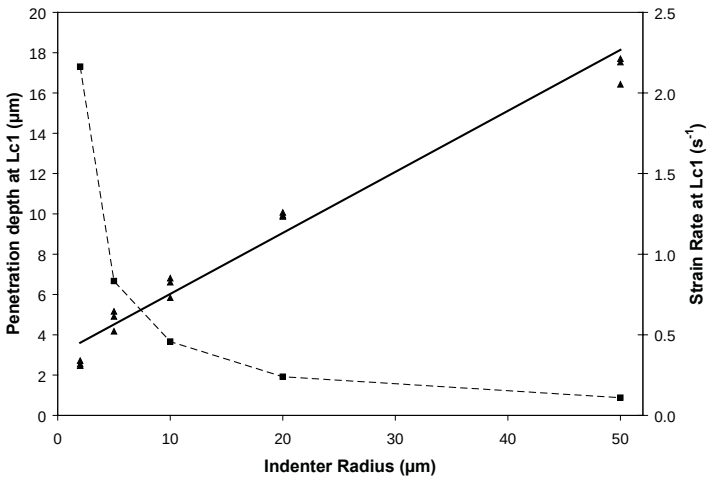

Figure 4: Penetration depth at the first critical failure point (Lc1) plotted against indenter radius for the 5 tested geometries. The corresponding strain rate at Lc1 is shown as a dotted line.

the influence of the cone above the actual radiused tip is significant. For example, for the 2 µm radius, the penetration depth at maximum load is approximately 40 µm so there is a much larger contact area from the indenter sidewalls than from the tip. Incidentally, the cone angle for all 5 indenters used in this study was 90°, this being the standard angle for scratch testing on polymeric coatings as detailed in ASTM D7187 [4].

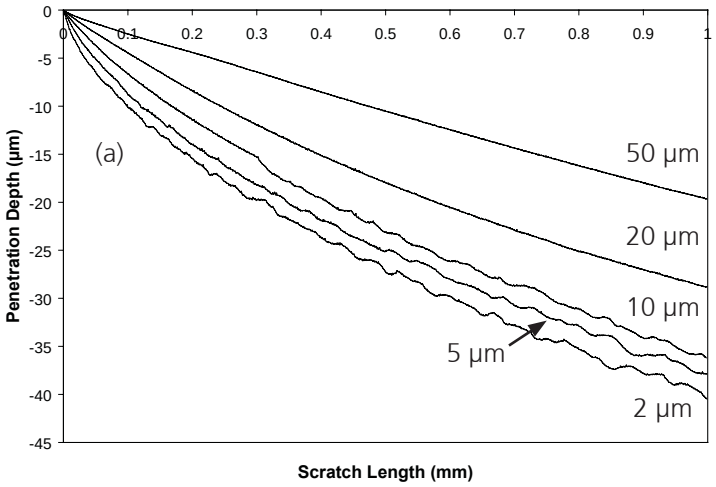

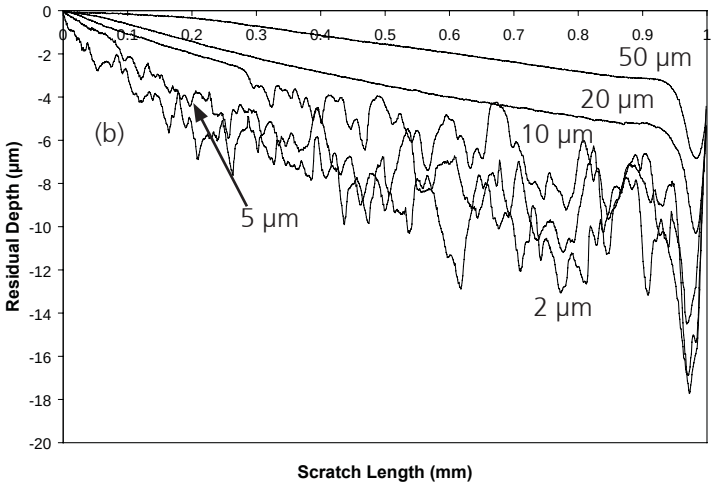

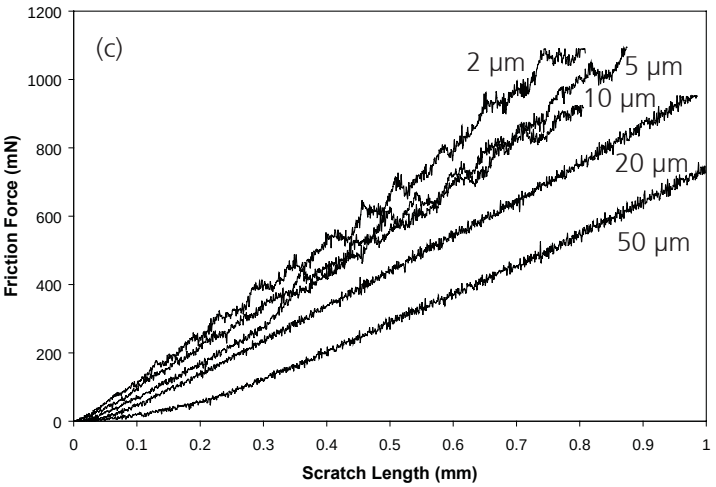

Figure 5: Overlays of (a) Penetration depth (Pd), (b) Residual depth (Rd) and (c) Friction Force (Ft) for the 5 tested indenter geometries. These data sets correspond to the scratches shown in Fig. 2

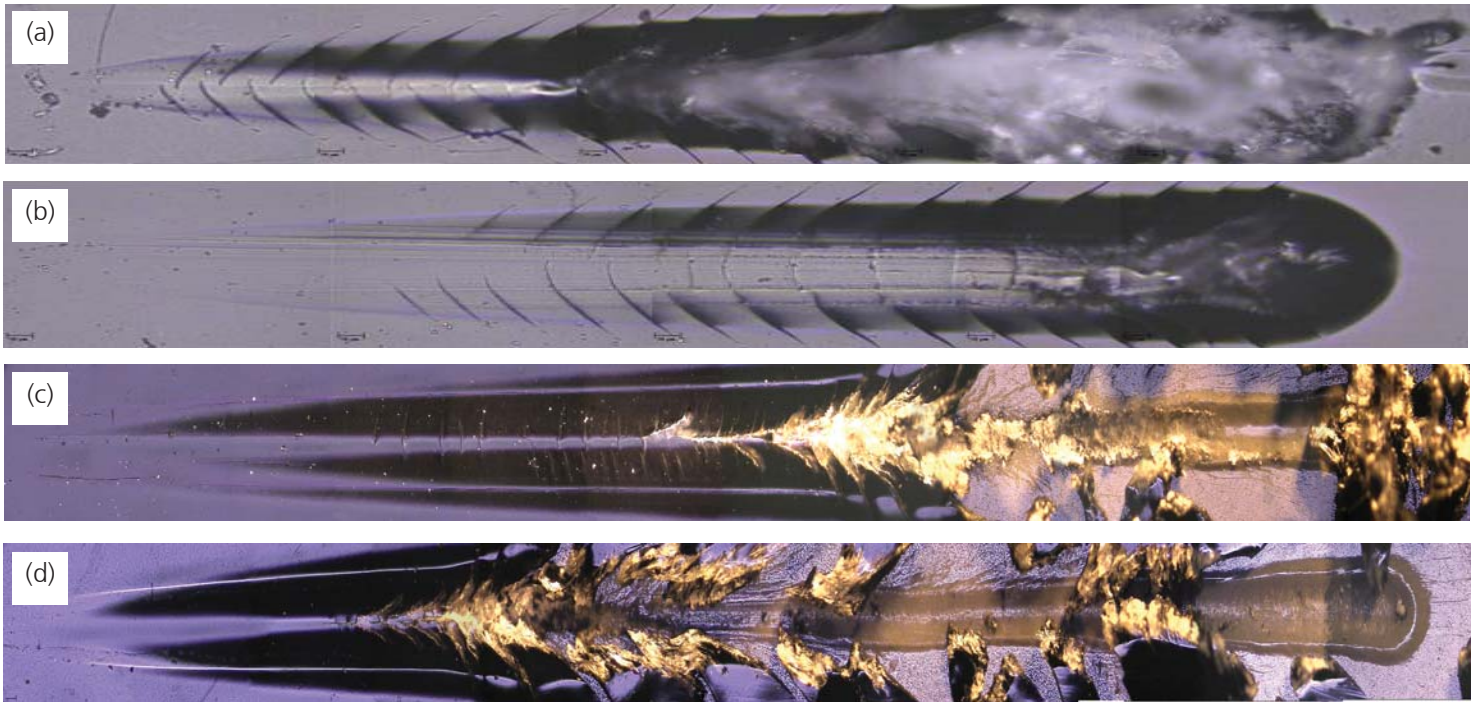

Figure 6: Scratches made on a GEN III polymer topcoat with the following spherical indenter radii and contact conditions; (a) 50 µm radius, 0.02 - 5 N applied load; (b) 100 µm radius, 0.02 - 5 N applied load; (c) 200 µm radius, 0.9 - 30 N applied load; (d) 500 µm radius, 0.9 - 100 N applied load

To complement the scratch tests shown in Fig. 2, some additional tests were performed on the same GEN III sample using indenters with radii from 50 - 500 µm and loads high enough to cause failure in the coating. For such a wide range of contact conditions both the Micro Scratch Tester (load range up to 30 N) and the Revetest (load range up to 200 N) were utilized. Sufficient load was applied with the 200 µm and 500 µm indenters to actually delaminate the polymer coating stack (topcoat and primer) from the underlying steel substrate. A typical example of a data set for the 200 µm radius is shown in Fig. 7 where Lc1 corresponds to first cracking in the coating and Lc2 corresponds to full delamination of the stack. This Lc2 value coincides with a sudden drop in the penetration depth and an increase in the friction force. At higher applied loads (around 23 N) the Pd signal flattens off due to the indenter having reached the steel substrate.

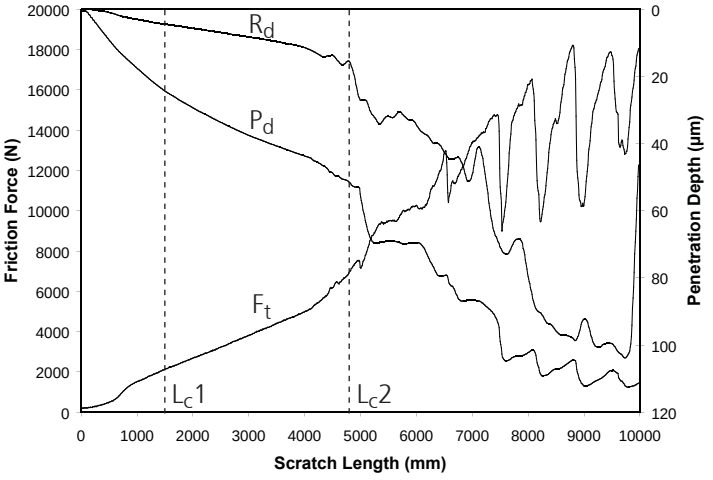

Figure 7: Revetest scratch tester results for a progressive load scratch (0.9 – 30 N) on a GEN III automotive polymer topcoat showing the penetration depth (Pd), residual depth (Rd) and friction force (Ft) signals. The onset of fracture (Lc1) and full delamination (Lc2) points are clearly visible (dotted lines) and correlate with the optical micrograph shown of the entire scratch in Fig. 6 (c). Indenter radius is 200 µm.

1. J. L. Courter, *Mar Resistance of Automotive Clearcoats: Relationship to Coating Mechanical Properties*, J. Coating Tech., 69 (1997) 57-63

2. L. Lin, G. S. Blackman and R. R. Matheson, *A new approach to characterize scratch and mar resistance of automotive coatings*, Progress in Organic Coatings, 40 (2000) 85-91

3. M. Osterhold and G. Wagner, *Methods for characterizing mar resistance*, Progress in Organic Coatings, 45 (2002) 365-371

4. ASTM D7187: *Test method for measuring mechanistic aspects of scratch/mar behavior of paint coatings by nanoscratching*

This Applications Bulletin is published quarterly and features interesting studies, new developments and other applications for our full range of mechanical surface testing instruments.

Editor: Dr Nicholas X. Randall

Should you require further information, please contact:

CSM Instruments
Rue de la Gare 4
CH-2034 Peseux
Switzerland

Tel: + 41 32 557 5600
Fax: +41 32 557 5610
info@csm-instruments.com
www.csm-instruments.com

621003.08v1 CSM Instruments / Printed in Switzerland